^{3}He polarization-dependent EPR frequency shifts of alkali-metal–^{3}He pairs

Earl Babcock,[1] Ian A. Nelson,[2] Steve Kadlecek,[3] and Thad G. Walker[1]
[1]*Department of Physics, University of Wisconsin–Madison, Madison, Wisconsin 53706, USA*
[2]*Department of Human Oncology, University of Wisconsin Medical School, Madison, Wisconsin 53792, USA*
[3]*Department of Radiology, University of Pennsylvania, Philadelpia, Pennsylvania 19104, USA*
(Received 8 September 2004; published 19 January 2005)

We present temperature-dependent measurements of the EPR frequency shifts for Na, K, and Rb interacting with polarized ^{3}He. K and Na frequency shifts were measured via comparison with Rb frequency shifts (well known at low temperatures) in Na-Rb-^{3}He and K-Rb-^{3}He spin-exchange cells. The lowered Rb vapor pressure of these "hybrid" spin-exchange cells also allowed us to extend the measured temperature dependence of the Rb EPR frequency shifts up to 350 °C. This work presents measurements of the EPR frequency shift for Na in ^{3}He and significantly extends the temperature range of previous Rb and K EPR frequency shift measurements. These results are critical to the performance of accurate ^{3}He EPR polarimetry in spin-exchange cells.

DOI: 10.1103/PhysRevA.71.013414 PACS number(s): 32.80.Bx, 32.30.Dx, 33.25.+k, 33.35.+r

Hyperpolarized ^{3}He has a wide variety of applied and fundamental research uses such as magnetic resonance imaging [1], spin-polarized targets [2], neutron spin filters [3], and precision measurements [4]. The most commonly used polarization technique for ^{3}He nuclei is spin-exchange optical pumping (SEOP). Nearly all SEOP experiments take advantage of high-power diode laser arrays (readily available at the Rb $D1$ wavelength) to optically pump a Rb vapor. The resulting spin polarization of the Rb valence electron is then transferred to the ^{3}He nucleus via a weak hyperfine coupling during spin-exchange collisions.

In practice, the polarization in many of these experiments is ultimately limited by the intrinsically low spin-exchange efficiency between Rb and ^{3}He [5]. The lighter alkali metals should provide much higher efficiencies; however, their resonances occur at less convenient wavelengths and their reduced hyperfine splitting also makes direct optical pumping much more difficult. Recently we have shown that one can greatly increase the overall efficiency of the spin-exchange process by using a mixture of K and Rb in a process called hybrid spin-exchange optical pumping (HySEOP) which takes advantage of both the experimental ease of using lasers at the Rb wavelength and the higher spin-exchange efficiency of K [6]. The efficiency could potentially be increased even further by using a Na-Rb mixture.

In studying SEOP and HySEOP, it is essential to have a robust and accurate measure of the degree of ^{3}He polarization. It is well established that the alkali-metal EPR frequency shift in the presence of polarized ^{3}He is a convenient tool for this purpose [7]. The EPR shift is largely caused by the Fermi-contact interaction $\alpha\mathbf{K}\cdot\mathbf{S}$ between the nuclear spin $\mathbf{K}$ of the noble gas nucleus of magnetic moment μ_K and the electron spin $\mathbf{S}$ of the alkali-metal atom. The measured shift is therefore qualitatively similar to the expected Zeeman interaction with the field produced by the bulk ^{3}He nuclear magnetism, but is larger by an enhancement factor, termed κ_0. Given that the enhancement arises from alkali-metal-electron–^{3}He nuclear overlap during binary collisions, it is not surprising that κ_0 is different for each alkali-metal partner, and is slightly temperature dependent [8]. Consequently, it must be measured for each alkali-metal species and over the range of temperatures required for HySEOP in order to perform ^{3}He polarimetry to the desired accuracy.

In this paper we present temperature-dependent measurements of κ_0 for K-^{3}He and Na-^{3}He. Additionally we greatly extend the measured temperature range of κ_0 for Rb-^{3}He. Our approach, which stems from the idea of HySEOP, is to use cells containing mixtures of Rb and another alkali metal. In these cells the κ_0 of the secondary alkali metal, K or Na, is determined directly from the measurable ratio of its frequency shift to those of Rb-^{3}He which are known to a high accuracy for temperatures from 120 to 175 °C. Consequently this procedure is insensitive to both absolute ^{3}He polarization and density, eliminating many sources of systematic error. We also note that the Na-Rb and K-Rb amalgams used for HySEOP have lowered vapor pressure curves as given by Raoult's law, and higher photon efficiency. Both of these effects allow us to maintain a highly polarized Rb vapor, and measure κ_0^{Rb}, at significantly higher temperatures than in a pure Rb optical pumping cell.

Our basic apparatus has been described in previous papers [6,9]. Spherical hybrid Na-Rb or K-Rb cells with nearly equal proportions of Na or K to Rb in the vapor phase are pumped using a diode laser tuned to the Rb $D1$ line. Rapid spin exchange among all of the alkali-metal atoms (regardless of species) ensures spin-temperature equilibrium and therefore equal polarizations. The spin polarization of the alkali-metal atoms is monitored using either transmission of the pumping light through the cell or by Faraday rotation of a weak diode laser (<5 mW) tuned slightly off the Rb $D2$ line.

EPR spectra are obtained by driving the K or Na and Rb resonances with a transverse rf magnetic field generated by a coil operated purposely far from any coil resonances (ensuring constant rf amplitude as a function of rf frequency), and sweeping the rf frequency. As the frequency becomes resonant with any one of the atomic resonances, the alkali metal becomes slightly depolarized, the transmission of the pump-

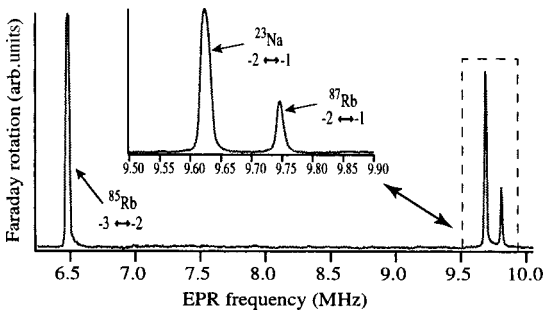

FIG. 1. EPR spectrum of ^{23}Na, ^{85}Rb, and ^{87}Rb. The notation $-2\leftrightarrow-1$ stands for the $m=-2$ to $m'=-1$ transition. Note if the alkali metal were not fully polarized the $m=-F+1\leftrightarrow m'=-F+2$ peaks would be visible; a full description of this is given in [9].

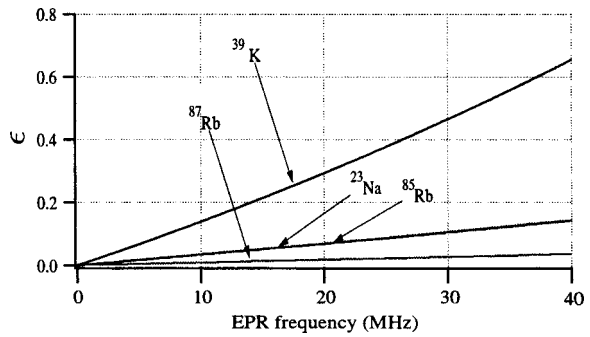

FIG. 2. Plot of the magnetic moment correction factor for the various alkali-metal isotopes as a function of the EPR frequency; note that for the special case of ^{85}Rb and ^{23}Na the correction factors follow each other to less than 0.1%.

ing light lessens, and the plane of polarization of the probe light changes. An example spectrum is shown in Fig. 1. Equivalently, one could obtain the spectra by holding the EPR frequency constant and sweeping the magnetic field. There is a tremendous amount of information in these spectra, but we focus in this paper on the dependence of the resonance frequencies on the nuclear spin polarization of the ^{3}He atoms.

The frequency shift of the alkali-metal $m=-F$ to $m=-F+1$ EPR line due the polarized ^{3}He in a cell of spherical geometry is [7]

$$\Delta\nu_0 = \frac{8\pi}{3}\frac{g_s\mu_B}{(2I+1)h}(1+\epsilon)\kappa_0\mu_K[\mathrm{He}]P_{\mathrm{He}}, \tag{1}$$

where ϵ is the magnetic moment correction factor, to be discussed further below, $\mu_K/h=1.6215$ kHz/G is the magnetic moment of ^{3}He, κ_0 is the frequency shift enhancement factor, μ_B is the Bohr magneton, g_s is the electron g factor, [He] is the ^{3}He density, P_{He} is the ^{3}He polarization, and I is the nuclear spin (5/2 for ^{85}Rb and 3/2 for ^{23}Na, ^{39}K, or ^{87}Rb). Romalis and Cates [7] measured the Rb-^{3}He frequency shift enhancement factor from 120 to 175 °C to be $\kappa_0=6.39+0.009\,34(T-200\ ^\circ\mathrm{C})$ with a precision of 1.5% for Rb, and Baranga *et al.* [5] measured the ratios of the K-Rb shifts to be $\kappa_0^{\mathrm{K}}=0.94\kappa_0^{\mathrm{Rb}}$ with a precision of 1%.

The magnetic moment correction factor ϵ arises from the nonlinear Zeeman effect. At low fields (<50 G) and for the $m=-F$ to $m=-F+1$ state used in this work, it is well approximated by

$$\epsilon = \frac{d\nu/dB|_B}{d\nu/dB|_0} - 1 = \frac{4I\Omega}{(2I+1)\delta\nu_{\mathrm{hfs}}} + \frac{6I(2I-1)\Omega^2}{(2I+1)^2\delta\nu_{\mathrm{hfs}}^2}, \tag{2}$$

where $\Omega=g_s\mu_B B/h$ and $\delta\nu_{\mathrm{hfs}}$ is the alkali-metal hyperfine splitting (462 MHz for ^{39}K, 1772 MHz for ^{23}Na, and 6835 MHz for ^{87}Rb). In the experiments described here, we find it necessary to work at sufficiently high magnetic field that the EPR spectra of the spin-3/2 isotopes of Na, K, and Rb are well resolved. This necessitates inclusion of the second term of Eq. (2) for accurate polarimetry. Figure 2 shows a plot of ϵ verses applied rf frequency. By numerical coincidence, if one keeps the rf frequency constant (i.e., changes B by $F_{^{23}\mathrm{Na}}/F_{^{85}\mathrm{Rb}}=2/3$), the correction factors for ^{85}Rb and ^{23}Na are the same to within less than 0.1%. Consequently the ratio of the κ_0's for ^{85}Rb and ^{23}Na can be measured directly without correcting for the magnetic moment.

For cells of nonspherical geometry an additional geometric correction factor κ' must be included to correct for the nonuniform magnetization of the cell caused by the ^{3}He nuclei. The total effective frequency shift enhancement factor κ_{eff} can be defined as [7]

$$\kappa_{\mathrm{eff}} = \kappa_0 + \kappa' = \kappa_0 + \frac{3}{8\pi}C(\vec{z}) - 1; \tag{3}$$

here $C(\vec{z})=B_z/M_{\mathrm{He}}$, where $M_{\mathrm{He}}=\mu_K[\mathrm{He}]P_{\mathrm{He}}$. $C(\vec{z})$ can be calculated using the method of the magnetic scalar potential [10]. For spherical cells $C(\vec{z})=8\pi/3$ and is uniform throughout the cell giving $\kappa'=0$. If we were to consider a cell defined by an ellipsoid of revolution with the major axis along $\vec{z}$, the direction of the applied holding field, $C(\vec{z})$ remains constant throughout the cell and becomes [11]

$$C(\vec{z}) = 4\pi\left[1 - \frac{1}{k^2-1}\left(\frac{k}{\sqrt{k^2-1}}\,\mathrm{arcosh}(k) - 1\right)\right], \tag{4}$$

where $k=a/b$ is the ratio of the lengths of the semimajor to semiminor axes. For geometries not definable as an ellipsoid, the field inside the cell is not uniform and one must average the geometric contribution along the detection volume as we did for a cylindrical geometry in [9]. For nearly all geometries of interest for SEOP $\kappa'<5\%$ of κ_0.

The Na-Rb cell was 7 cm in diameter and made of GE180 glass. It was filled with 2 bar of ^{3}He and 50 Torr of N_2, as measured at room temperature. We estimate that approximately 500 mg Na was distilled into it, followed by a trace of Rb to obtain about a 1:1 Na:Rb ratio in the vapor phase. The procedure for obtaining experimentally desirable alkali-metal ratios in the vapor phase is described in [6]. Although Na reactions with the glass formed an opaque brown coating in this cell after a few weeks, we were still able to polarize the alkali metal sufficiently to get ^{3}He polarizations on the order of 40–50 %. The K-Rb cell was 3.5 cm in diameter, also constructed of GE180 glass. It was filled with 3.3 bar ^{3}He, 80 Torr of N_2, as measured at room temperature, and had roughly a 10:1 K:Rb ratio in the metal

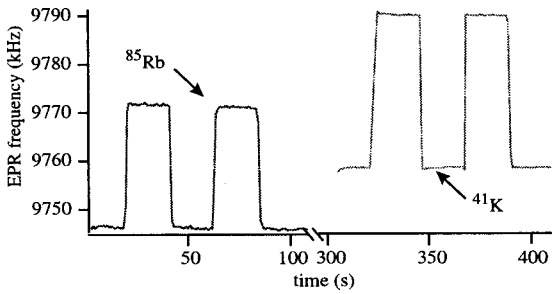

FIG. 3. Typical EPR frequency data for a series of four AFP reversals for ^{85}Rb followed by ^{41}K. The break in the graph indicates the pause to take FID data and to change the field from 21 G for the Rb data to 14 G for the K data.

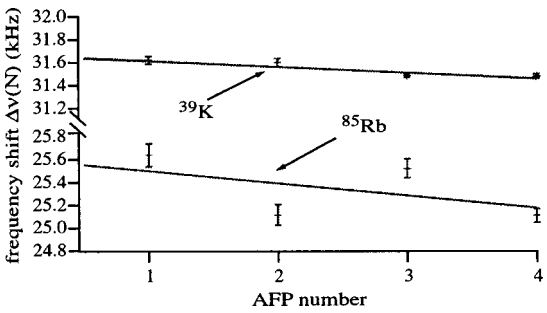

FIG. 4. Difference of the adjacent EPR frequencies of the AFP reversals shown in Fig. 3 with fits to determine the initial value of the frequency shift $\Delta\nu$. Note that the scatter in the data is caused by field fluctuations.

phase to obtain approximately a 1.5:1 K:Rb ratio in the vapor phase. In this cell we could obtain as high as 75–80 % ^{3}He polarization. We also had a twin 3.5-cm-diameter pure Rb cell that we used for additional Rb frequency shift measurements at temperatures below 200 °C.

We measure the frequency shifts by using a 9–14 MHz voltage controlled oscillator (Connor-Winfield model No. PL14R3) to drive a rf coil which was locked to the EPR frequency using a simple proportional-integral feedback circuit with a lock-in output to create a dispersion signal. The ^{3}He spin was then reversed (from spin up to spin down, or vice versa) using adiabatic fast passage (AFP), while recording the EPR frequency using a digital counter. Note that the corresponding total frequency difference of the monitored EPR peak is $2\Delta\nu_0$ because the ^{3}He polarization is being changed from $+P_{\mathrm{He}}$ to $-P_{\mathrm{He}}$. The magnetic field was not stabilized for the experiment. There was a small loss of 0.5% per AFP reversal that was corrected for by taking four successive EPR spectra in rapid order, pausing between spectra for about 20 s to acquire frequency data and to perform AFP to reverse the ^{3}He spins. Figure 3 shows a typical data set. The absolute value of the difference in frequency between adjacent EPR spectra $[\Delta\nu(N)]$ was taken and plotted versus the counting number of the AFP reversal (N). These data were then fitted to the function

$$\Delta\nu(N) = 2\Delta\nu_0\left[1 - \left(N - \frac{1}{2}\right)\varepsilon\right] \tag{5}$$

to extrapolate the initial frequency shift value $\Delta\nu_0$. This fit function results from the first-order terms of an expansion about $\varepsilon = 0$ for the loss between two adjacent spectra. We note that the AFP loss coefficient ε determined from the EPR spectra was in agreement with NMR free induction decay (FID) data taken directly before and after the spectra. The spectra of both alkali metals (Na-Rb or K-Rb) were taken in rapid succession for each temperature with FID data taken in between. The values of $\Delta\nu_0$ were then normalized using the FID amplitudes taken directly before the respective EPR scan. A sample of the data is shown in Fig. 4.

Typical values of the measured frequency shifts $\Delta\nu(N)$ ranged from around 12 kHz for the ^{23}Na and 16 kHz for the ^{87}Rb in the Na-Rb cell and 30–60 kHz for the ^{39}K and ^{87}Rb in the K-Rb cell. We chose a field high enough that the differential Zeeman splitting of the $I=3/2$ isotopes was greater than the EPR shifts, and high enough to give adequate resolution of the spectra (>100 kHz). We found a field of 14 G corresponding to an unshifted EPR frequency of 9.8 MHz to be more than adequate. Figure 1 shows a typical EPR spectrum for our Na-Rb cell.

In order to measure the temperature dependence of κ_0 for Rb, we first verified that the polarization measurement via the NMR FID amplitude was a temperature-independent reference. We placed a high-Q FID pickup coil outside of our oven, approximately 2 cm away from the cell, and cooled it so that its temperature remained constant. We then looked for any cell temperature dependence by quickly changing the temperature of the cell from 350 °C down to 150 °C and back up to 350 °C in 50 °C steps and observing the FID amplitude at each step. This process took a total time of less than 1.5 h. Note the Na-Rb cell used for this measurement had a ^{3}He wall relaxation time constant of 254 h, so by polarizing the ^{3}He in this cell to its maximum value and maintaining constant alkali-metal polarization by optical pumping (as monitored via rf spectroscopy), we were able to ensure that the ^{3}He polarization did not vary significantly during this measurement. The initial and final FID amplitudes at 350 °C were equal within the statistical errors. We determined the FID amplitudes to have a temperature coefficient of $0.0\% \pm 0.5\%$ from 150 to 350 °C, limited by the uncertainty in the NMR pulses themselves.

The absolute temperature of the cell was measured directly with a calibrated optical pyrometer 20 cm above the cell. The optical pyrometer (Exergen model No. Irt/c.10) was calibrated with an Omega WT-J thermocouple which was temporarily placed on the cell under the same conditions as during optical pumping for the calibration. The thermocouple was removed for the actual optical pumping.

After completing the data set with each cell we normalized the Rb frequency shifts to the FID amplitudes and fitted the result as a function of temperature. We then used the well tested value of κ_0^{Rb} given by [7] to scale the value of our fit at 170 °C. We note that this calibration automatically compensates for any errors in the ^{3}He polarization introduced by the uncertainty in the ^{3}He density by solving for the product of all of the constants in Eq. (1). Once the Rb frequency shifts were determined over our entire temperature range, we then solved for the frequency shifts for Na and K. We did

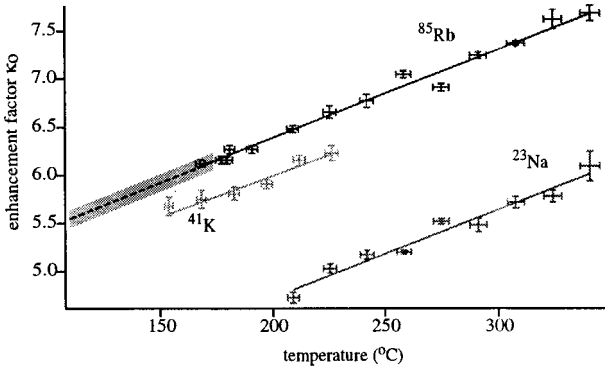

FIG. 5. Experimental results for the determination of κ_0 as a function of temperature. The top line is ^{85}Rb, the middle line is ^{39}K, and the bottom line is ^{23}Na. The dotted line with error (shaded region) is the previous measurement of κ_0 for lower temperatures by Romalis and Cates [7].

this by normalizing the Na and K shifts to the FID amplitudes, correcting for ϵ and I, and taking the ratios of these shifts to those of the normalized Rb shifts at the same temperature. The data from these measurements are shown in Fig. 5. The fit values for Rb, K, and Na from this work are given below;

$$\kappa_0^{\mathrm{Rb}} = 6.39 + 0.009\,14[T - 200(^\circ\mathrm{C})], \tag{6}$$

$$\kappa_0^{\mathrm{K}} = 5.99 + 0.0086[T - 200(^\circ\mathrm{C})], \tag{7}$$

$$\kappa_0^{\mathrm{Na}} = 4.84 + 0.009\,14[T - 200(^\circ\mathrm{C})]. \tag{8}$$

The fit of the Rb data indicates that the temperature coefficient for κ_0^{Rb} is consistent with the value of [7] up to 350 °C. Also we note that the values of the ratios of κ_0^{Na} and κ_0^{K} to κ_0^{Rb} given in Table I agree very well with the theoretical predictions of [12] at 100 °C, and with prior measurements of [5] under optical pumping conditions. The values of the EPR frequency shifts for several of the alkali-metal–noble-gas pairs have been previously measured [7,8,13] with results summarized in Table II.

The statistical errors for the values of the κ_0's at 200 °C are 1% for ^{23}Na and 0.5% for ^{39}K. The statistical errors in the temperature coefficients κ_0' are 6% for ^{23}Na, 15% for ^{39}K, and 2% for ^{85}Rb. The fractional errors in the temperature dependence are larger for ^{23}Na and ^{39}K for statistical reasons, but since the temperature dependence represents only a small fractional correction to κ_0, the error induced by using these values of κ_0 over the measured temperature range is dominated by the errors in the κ_0's themselves. The errors in the temperature coefficients are provided in order to allow one to estimate the error that would be introduced if one were to extrapolate far beyond the measured temperature range.

TABLE I. Ratios of the experimental and theoretical ^{3}He frequency shift enhancement factors. The 100 °C experimental values are extrapolated from the measured temperature dependence.

	Temperature (°C)	$\kappa_0^{\mathrm{Na}}/\kappa_0^{\mathrm{Rb}}$	$\kappa_0^{\mathrm{K}}/\kappa_0^{\mathrm{Rb}}$
Walker [12] (theory)	100	0.74	0.97
This work	100	0.696±0.016	0.938±0.024
This work	200	0.739±0.007	0.937±0.005
Baranga *et al.* [5]	200		0.94±0.01

TABLE II. Known experimental values of κ_0 and known temperature coefficients κ_0' with theoretical calculations of Walker [12] at 100 °C. Here the κ_0 for a particular temperature is given by $\kappa_0(T) = \kappa_0(T_{\mathrm{ref}}) + \kappa_0'(T - T_{\mathrm{ref}})$ where the reference temperature of the measurement, T_{ref}, is given in parentheses.

Pair	κ_0	κ_0'	Theory[a]
NaHe[b]	4.72±0.09 (200 °C)	0.00914±0.00056	6.5
KHe[c]	6.01±0.11 (200 °C)		8.5
KHe[b]	5.99±0.11 (200 °C)	0.0086±0.0020	8.5
ReHe[d]	6.15±0.09 (175 °C)	0.00934±0.00014	8.8
RbHe[b]		0.00916±0.00026	8.8
RbNe[e]	32.0±2.9 (128 °C)		38
RbKr[f]	270±95 (90 °C)		280
RbXe[f]	644±269 (80 °C)		730

[a]Reference [12].
[b]This work.
[c]Reference [5].
[d]Reference [7].
[e]Reference [13].
[f]Reference [8].

The sources of random error are the FID statistical error (0.5%), repeatability of the optical pyrometer (1%), and frequency shift statistical error (1%), which resulted mainly from field fluctuations. Possible systematic errors include the temperature calibration with the thermocouple (0.75%), error in the temperature dependence of the NMR FID amplitudes (0.5%), and calibration to the previous κ_0^{Rb} measurement (1.5%) for a total of 1.8%. An important point about the methods used here is that the absolute He polarization and density cancel out in the κ_0 ratio measurements, so no uncertainty arises from these sources.

The cells used in this work were nearly spherical, and κ' was taken to be zero. The diameters of the cells were measured to vary by less than 1 mm; thus for the K-Rb cell if one assumed it to be an ellipsoid of revolution the maximum error induced in the measurement of P_{He} would be 1.6%. For the Na-Rb cell this error would be 0.6%. Since our method relies on the measurement of the ratios of the frequency shifts for Na or K to those of Rb in the same cell, the systematic error induced in the measured value of κ_0 by $\kappa' \neq 0$ is suppressed by $(1-R)\kappa'$ where R is the ratio of κ_0^{K} or κ_0^{Na} to κ_0^{Rb}. Since $R \approx 0.75$ for Na-Rb and $R \approx 0.95$ for K-Rb the induced error in κ_0 from this source becomes negligible.

An additional correction to κ' could also result from the volume of the cell's stem. For both of our cells the volume of the stem was small, less than 1 cm^3, for the Na-Rb cell and

less than 0.1 cm^3 for the K-Rb cell. Approximating the field from the polarized ^{3}He atoms in the stem as a dipole we obtained an additional correction to $\kappa' \ll 1\%$.

With the increasing interest in alkali metals other than Rb for SEOP [5,6,14,15], having precision EPR polarimetry will be very important for future developments. In addition, the method used here should be extendable to the important case of ^{129}Xe, where κ_0 and its molecular counterpart κ_1 are only known to 50% accuracy [8].

This work was partially supported by the NSF and DOE Grant No. DE-FG02-99ER40410.

[1] M. S. Albert, G. D. Cates, B. Driehuys, W. Happer, B. Saam, C. S. Springer, Jr., and A. Wishnia, Nature (London) **370**, 199 (1994).
[2] W. Xu *et al.*, Phys. Rev. Lett. **85**, 2900 (2000).
[3] B. Chann, E. Babcock, L. W. Anderson, T. G. Walker, W. C. Chenn, T. B. Smith, A. K. Thompson, and T. R. Gentile, J. Appl. Phys. **94**, 6908 (2003).
[4] D. Bear, R. E. Stoner, R. L. Walsworth, V. A. Kostelecky, and C. D. Lane, Phys. Rev. Lett. **85**, 5038 (2000).
[5] A. B. Baranga, S. Appelt, M. V. Romalis, C. J. Erickson, A. R. Young, G. D. Cates, and W. Happer, Phys. Rev. Lett. **80**, 2801 (1998).
[6] E. Babcock, I. Nelson, S. Kadlecek, B. Driehuys, L. W. Anderson, F. W. Hersman, and T. G. Walker, Phys. Rev. Lett. **91**, 123003 (2003).
[7] M. V. Romalis and G. D. Cates, Phys. Rev. A **58**, 3004 (1998).
[8] S. R. Schaefer, G. D. Cates, Ting-Ray Chien, D. Gonatas, W. Happer, and T. G. Walker, Phys. Rev. A **39**, 5613 (1989).
[9] B. Chann, E. Babcock, L. W. Anderson, and T. G. Walker, Phys. Rev. A **66**, 032703 (2002).
[10] J. D. Jackson, *Classical Electrodynamics* (Wiley, New York, 1999), p. 196.
[11] R. Skomski and J. M. D. Coey, *Permanent Magnetism* (Institute of Physics Publishing, Bristol, 1999), p. 55.
[12] T. G. Walker, Phys. Rev. A **40**, 4959 (1989).
[13] R. E. Stoner and R. L. Walsworth, Phys. Rev. A **66**, 032704 (2002).
[14] Guodong Wang, Wenjin Shao, and Emlyn W. Hughes, Phys. Rev. A **68**, 065402 (2003).
[15] P. I. Borel, L. V. Sogaard, W. E. Svendsen, and N. Andersen, Phys. Rev. A **67**, 062705 (2003).